ISSN 1392 - 1207. MECHANIKA. 2013 Volume 19(5): 544-548

Dynamics and simulation of biorobotic UUV

DU Xiao-xu*, SONG Bao-wei, PAN Guang*****
**Northwestern Polytechnical University, Youyi Xilu 127,710072 Xi'an, China, E-mail: nwpudxx@163.com*
***Northwestern Polytechnical University, Youyi Xilu 127,710072 Xi'an, China, E-mail: songbaowei@nwpu.edu.cn*
****Northwestern Polytechnical University, Youyi Xilu 127,710072 Xi'an, China, E-mail: panguang601@163.com*

crossref http://dx.doi.org/10.5755/j01.mech.19.5.5531

1. Introduction

Natural swimmers have evolved to beautifully utilize physical principles from unsteady hydrodynamics to achieve high maneuverability and efficiency. Man-made unmanned underwater vehicles (UUVs), on the other hand, have been conceived and operated for decades to either remain safely within the realm of steady hydrodynamics – where the design of vehicle body, actuation mechanisms, and control system is simpler to understand and implement – or to avoid the issue altogether by using a number of thrusters to push an arbitrarily-shaped body through the water. This has often resulted in efficient cruising, but not in efficient maneuvering [1].

A number of numerical investigations about the dynamics of the biorobotic UUV. Mukund Narasimhan and Sahjendra N. Singh [2, 3] provided the open-loop control and feedback linearizing yaw plane control of a multifin biorobotic rigid underwater vehicle. WANG Zhao-li et al. [4] provided the Hydrodynamic analysis of the pectoral-fins in viscous flows, and LAO Yi-jia et al. [5] and LIU Zhen et al. [6] gives some experimental results of oscillating flexible caudal fin. Haibin Xie et al. [7] and Shao-bo Yang et al. [8] studied dynamic and kinematics of the robotic fish.

This paper presents an innovative propulsion system approach for a new vehicle, resulting in efficient maneuvering through the exploitation of unsteady hydrodynamics. The vehicle swims by coordinating the motion of four biology-inspired high-lift flapping hydrofoils that are attached to its rigid hull. Because of this connection to biology, this vehicle has been named biorobotic UUV. Section 2 introduces the dimensional motion model of biorobotic UUV. Section 3 presents the model for fluid dynamics of flapping hydrofoil. Section 4 provides the simulation results of the motion of the biorobotic UUV which is propelled and controlled by four flapping hydrofoils. Finally, section 5 draws conclusions.

2. Dimensional motion model of biorobotic UUV

A earth-fixed frame $S_E(o, x_0, y_0, z_0)$, and a Biorobotic UUV body-fixed frame $S_B(B, x, y, z)$, as shown in Fig. 1, are defined, and their transform matrixes are $\boldsymbol{C}_E^B$, and $\boldsymbol{C}_B^E$. The Biorobotic UUV's velocity vector is considered to be $\boldsymbol{V} = \left[\boldsymbol{v}^{\mathrm{T}}, \boldsymbol{\omega}^{\mathrm{T}}\right]^T$, $\boldsymbol{v} = \left[v_x, v_y, v_z\right]^T$, $\boldsymbol{\omega} = \left[\omega_x, \omega_y, \omega_z\right]^T$, and the earth-fixed position/orientation vector is $\boldsymbol{R} = \left[\boldsymbol{r}^{\mathrm{T}}, \boldsymbol{\Theta}^{\mathrm{T}}\right]^T$, $\boldsymbol{r} = \left[x_0, y_0, z_0\right]^T$, $\boldsymbol{\Theta} = \left[\theta, \psi, \varphi\right]^T$. The Dimensional Motion Model of Biorobotic UUV is built, as shown in Eqs. (1) and (2) [2, 9-10]. And a detailed explanation of this can be found in the literature [9] and [10].

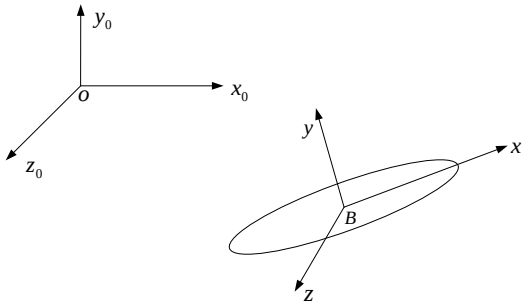

Fig. 1 Biorobotic UUV frames

$$
\begin{cases}
m\left[\dot{v}_x - v_y\omega_z + v_z\omega_y - x_c\left(\omega_y^2 + \omega_z^2\right) + y_c\left(\omega_x\omega_y - \dot{\omega}_z\right) + z_c\left(\omega_x\omega_z + \dot{\omega}_y\right)\right] = F_x \\
m\left[\dot{v}_y + v_x\omega_z - v_z\omega_x + x_c\left(\omega_x\omega_y + \dot{\omega}_z\right) - y_c\left(\omega_x^2 + \omega_z^2\right) + z_c\left(\omega_y\omega_z - \dot{\omega}_x\right)\right] = F_y \\
m\left[\dot{v}_z - v_x\omega_y + v_y\omega_x + x_c\left(\omega_x\omega_z - \dot{\omega}_y\right) + y_c\left(\omega_y\omega_z + \dot{\omega}_x\right) - z_c\left(\omega_x^2 + \omega_y^2\right)\right] = F_z \\
J_{xx}\dot{\omega}_x + \left(J_{zz} - J_{yy}\right)\omega_y\omega_z + J_{xy}\left(\omega_x\omega_z - \dot{\omega}_y\right) - J_{yz}\left(\omega_y^2 - \omega_z^2\right) - J_{xz}\left(\omega_x\omega_y + \dot{\omega}_z\right) + \\
\quad + m\left[y_c\left(\dot{v}_z - v_x\omega_y + v_y\omega_x\right) - z_c\left(\dot{v}_y + v_x\omega_z - v_z\omega_x\right)\right] = M_x \\
J_{yy}\dot{\omega}_y + \left(J_{zz} - J_{yy}\right)\omega_x\omega_z - J_{xy}\left(\omega_x\omega_z - \dot{\omega}_y\right) - J_{yz}\left(\omega_y^2 - \omega_z^2\right) - J_{xz}\left(\omega_x\omega_y + \dot{\omega}_z\right) + \\
\quad + m\left[x_c\left(\dot{v}_z - v_x\omega_y + v_y\omega_x\right) - z_c\left(\dot{v}_x - v_y\omega_z + v_z\omega_y\right)\right] = M_y \\
J_{zz}\dot{\omega}_z + \left(J_{yy} - J_{xx}\right)\omega_x\omega_z - J_{xy}\left(\omega_x^2 - \omega_y^2\right) - J_{yz}\left(\omega_x\omega_z + \dot{\omega}_y\right) + J_{xz}\left(\omega_y\omega_z - \dot{\omega}_x\right) + \\
\quad + m\left[x_c\left(\dot{v}_y + v_x\omega_z - v_z\omega_x\right) - y_c\left(\dot{v}_x - v_y\omega_z + v_z\omega_y\right)\right] = M_z
\end{cases}
\tag{1}
$$

$$\begin{bmatrix}\dot{x}\\ \dot{y}\\ \dot{z}\\ \dot{\varphi}\\ \dot{\theta}\\ \dot{\psi}\end{bmatrix}=\begin{bmatrix} v_x\cos\theta\sin\psi+v_z\left(\cos\varphi\sin\psi+\sin\varphi\sin\theta\cos\psi\right)\\ \quad+v_y\left(\sin\varphi\sin\psi-\cos\varphi\sin\theta\cos\psi\right)\\ v_x\sin\theta-v_z\sin\varphi\cos\theta+v_y\cos\varphi\cos\theta\\ -v_x\cos\theta\sin\psi+v_z\left(\cos\varphi\cos\psi-\sin\varphi\sin\theta\sin\psi\right)\\ \quad+v_y\left(\sin\varphi\cos\psi+\cos\varphi\sin\theta\sin\psi\right)\\ \omega_x-\omega_y\cos\varphi\tan\theta+\omega_z\sin\varphi\tan\theta\\ \omega_z\cos\varphi+\omega_y\sin\varphi\\ \left(-\omega_z\sin\varphi+\omega_y\cos\varphi\right)/\cos\theta\end{bmatrix} \tag{2}$$

The right hand term in Eq. (1) is the vector of external forces and moments, such as weight, buoyant, fluid dynamics which produced by the motion of UUV, and disturbed force which produced by the environment. In this paper, we suppose that the Biorobotic UUV motions in the enough deep, enough big and enough quiescent water, so the disturbed force which produced by the environment is ignorable. And the fluid dynamics which produced by the motion of UUV can be described by the mass forces and drag forces of the main body and the fluid dynamics of the flapping hydrofoil [11]. The mass forces and drag forces of the main body can be computed by the model which is detailed described in the literature [1] and [10]. And the model of the fluid dynamics of the flapping hydrofoil is built in the next section.

3. Fluid dynamics of flapping hydrofoil

According to Green theorem, the perturbation velocity potential $\Phi(t)$ in inviscid, incompressible, and irrotational flow with non-uniform velocity $\boldsymbol{V}(x,y,z,t)$ of an arbitrary field point $P(x,y,z,t)$ can be expressed as an integral on the boundary surface of flow field S, which is composed of flapping hydrofoil surface S_B, wake surface S_W and outer control surface S_∞, [11-13]:

$$2\pi\Phi(P,t)-\iint_S\left[\begin{array}{l}\Phi(Q,t)\dfrac{\partial}{\partial n_Q}\left(\dfrac{1}{R(P,Q)}\right)-\\ -\dfrac{\partial\Phi(Q,t)}{\partial n_Q}\dfrac{1}{R(P,Q)}\end{array}\right]dS=0, \tag{3}$$

where $R(P,Q)$ is the distance between field point $P(x,y,z,t)$ and boundary point $Q(x_0,y_0,z)$, $\dfrac{\partial}{\partial n_Q}$ is normal derivative to S at point Q.

The perturbation potential $\Phi(t)$ should satisfy the following boundary conditions:

$$\nabla\Phi(t)\to 0,\ S_\infty\to\infty; \tag{4}$$

$$\frac{\partial\Phi(t)}{\partial n_Q}=-\boldsymbol{V}_0(x,y,z,t)\times\boldsymbol{n}_Q \text{ on } S_B; \tag{5}$$

$$P^+-P^-=0; \tag{6}$$

$$\left(\frac{\partial\Phi(t)}{\partial n_{Q_t}}\right)^+-\left(\frac{\partial\Phi(t)}{\partial n_{Q_t}}\right)^-=0 \text{ on } S_W, \tag{7}$$

where, $\boldsymbol{n}_Q$ is unit normal vector on the flapping hydrofoil surface, Q_t is the point on the wake surface and superscripts + and - are used respectively to mark the values of upper and lower sides of wake.

Thus the integral Eq. (3) can be written as [11]:

$$\begin{aligned}2\pi\Phi(P,t)&-\iint_{S_B}\Phi(Q,t)\frac{\partial}{\partial n_{Q_t}}\left(\frac{1}{R(P,Q)}\right)dS-\\ &-\iint_{S_W}\Delta\Phi(Q_t,t)\frac{\partial}{\partial n_{Q_t}}\frac{1}{R(P,Q_t)}dS-\\ &-\iint_{S_B}\left(\boldsymbol{V}(t)\times\boldsymbol{n}_Q\right)\left(\frac{1}{R(P,Q)}\right)dS=0,\end{aligned} \tag{8}$$

where $\Delta\Phi$ is the potential jump across the wake surface, which can be expressed by:

$$\Delta\Phi(t)=\Phi(t)^+-\Phi(t)^-. \tag{9}$$

For the unsteady problem, the velocity potential $\Phi(t)$ changes with the time. And combining the Kutta pressure condition:

$$(\Delta p)_{TE}(t)=p_{TE}^+(t)-p_{TE}^-(t)=0, \tag{10}$$

the integral Eq. (8) can be uniquely solved by means of numerical iterative method.

The perturbation velocities $\boldsymbol{V}(x,y,z,t)$ on the flapping hydrofoil surface are evaluated by differentiating the velocity potential on the flapping hydrofoil surface. So the total velocity is:

$$\boldsymbol{V}_t(x,y,z,t)=\boldsymbol{V}_0(x,y,z,t)+\boldsymbol{V}(x,y,z,t). \tag{11}$$

By Bernoulli's theorem the pressure on the flapping hydrofoil surface can be expressed as [12]

$$p(t)=p_0+\frac{1}{2}\rho\left[\left|\boldsymbol{V}_0(t)\right|^2-\left|\boldsymbol{V}_t(t)\right|^2\right]-\rho\frac{\partial\Phi(t)}{\partial t}. \tag{12}$$

The hydrodynamic characteristics are obtained by integrating the pressure on the flapping hydrofoil surface.

Eq. (8) is a integral for determining the potential

Φ on the flapping hydrofoil surface S_B and the normal derivative $\frac{\partial}{\partial n_Q}$ on flow field S at point Q. The flapping hydrofoil surface S_B and the wake surface S_W can be individually divided into certain element with the number of N_B or N_W. And each element has a certain serial number N_j $\left(j=1,2,\cdots,N_B+N_W\right)$. The field point $P_i(x_i,y_i,z_i)$ is placed on the shape center of every element, and the term $\Phi(P)$ in Eq. (8) merges into other terms. The potential at the nodes of elements can be tackled by employing the following

$$\begin{aligned}\Phi\left(P_i^{node}\right)=&\sum_{j=1}^{N_B}\frac{\Phi_j}{2\pi}\iint_{S_{Bj}}\frac{\partial}{\partial n_Q}\left(\frac{1}{R_{ij}}\right)dS+\\&+\sum_{j=N_B+1}^{N_B+N_W}\frac{\Phi_j}{2\pi}\iint_{S_{Bj}}\frac{\partial}{\partial n_Q}\left(\frac{1}{R_{ij}}\right)dS+\\&+\sum_{j=1}^{N_B}\frac{1}{2\pi}\iint_{S_{Bj}}\Phi_j\frac{\partial}{\partial n_Q}\left(\frac{1}{R_{ij}}\right)dS.\end{aligned}\tag{13}$$

4. Simulation

For demonstration of the model of biorobotic UUV dimensional motion and the model for fluid dynamics of flapping hydrofoil, a numerical example of the motion of the biorobotic UUV is presented. The biorobotic UUV has a compressed body propelled and controlled by four flapping hydrofoils. The four flapping hydrofoils' collocation on the UUV is shown in Fig. 2. And the biorobotic UUV which was simulated in this paper has specifications of 10.0 m length, 3200 kg weight, 1.5 m wide.

Each flapping hydrofoil is assumed to undergo a flapping motion described as [14]:

$$\theta_i=A_i\sin\left(2\pi f_i t+\phi_i\right)+\theta_i^0,\tag{14}$$

where θ_i is the flapping angle of the ith hydrofoil, A_i is the crest value of θ_i, ϕ_i is the original phase angle, and θ_i^0 is the central angle of the flapping hydrofoil.

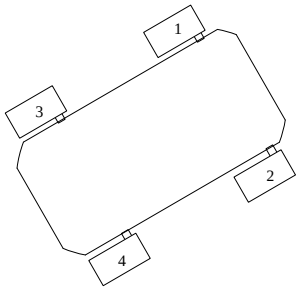

Fig. 2 Flapping hydrofoils' collocation on the biorobotic UUV

According the fluid dynamics model of flapping hydrofoil, the fluid dynamics of flapping hydrofoil was calculated. The Fig. 3 is the contours of pressure.

The biorobotic UUV can complete the motion of change depth through changing the central flapping angles of the two frontal flapping hydrofoils. And the biorobotic UUV also can complete the motion of change depth through changing the central flapping angles of all frontal flapping hydrofoils. The two motions of change depth are simulated.

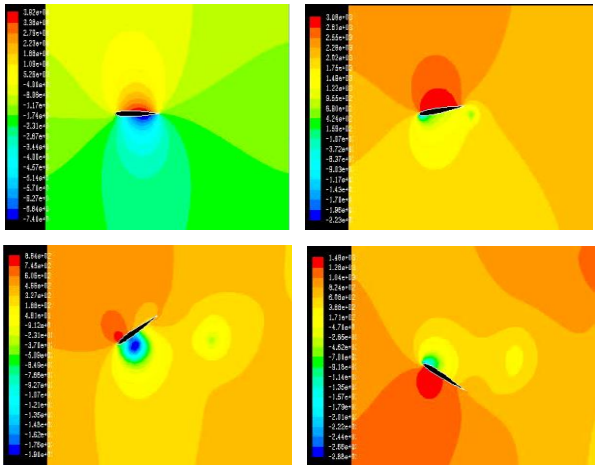

Fig. 3 Pressure contours of flapping hydrofoil

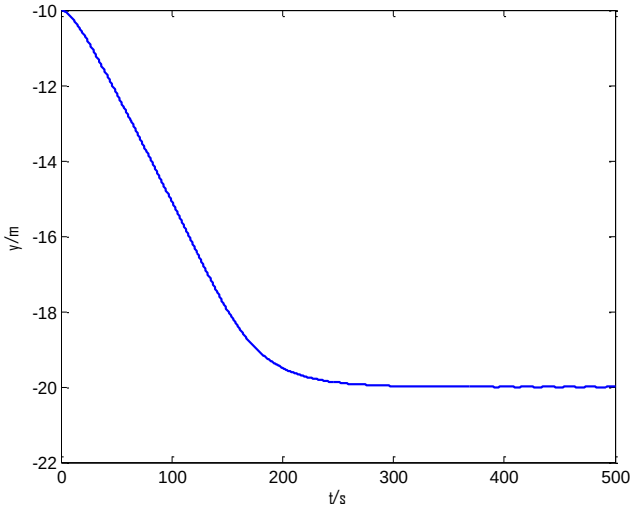

Fig. 4 Depth curve when changing depth through changing the central flapping angles of the two frontal flapping hydrofoils

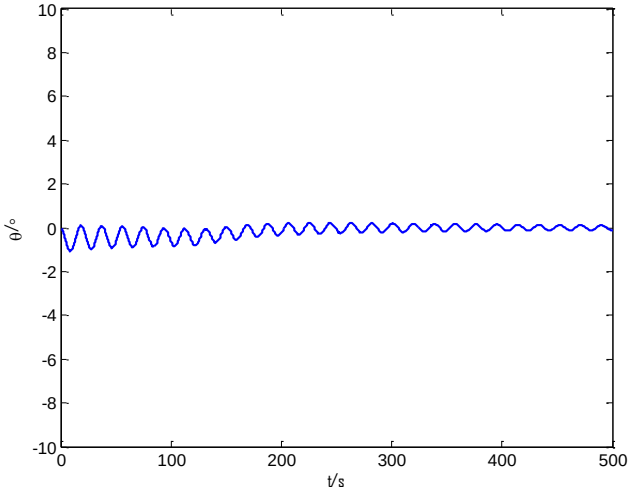

Fig. 5 Pitching angle curve when changing depth through changing the central flapping angles of the two frontal flapping hydrofoils

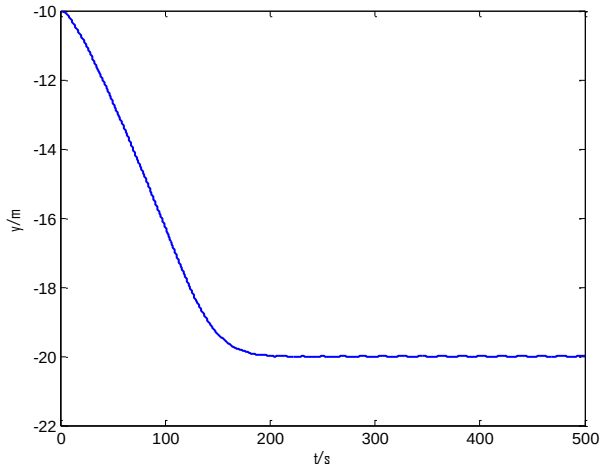

Fig. 6 Depth curve when changing depth through changing the central flapping angles of all frontal flapping hydrofoils

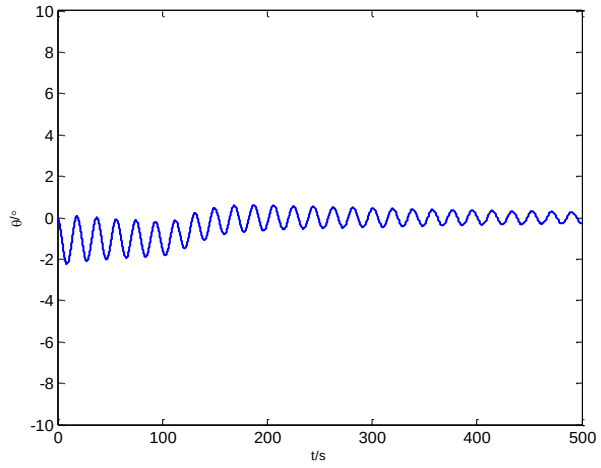

Fig. 7 Pitching angle curve when changing depth through changing the central flapping angles of all frontal flapping hydrofoils

The Fig. 4 is the depth curve and pitching angle curve when the biorobotic UUV changing depth form 10 to 20 m through changing the central flapping angles of the two frontal flapping hydrofoils. And the Fig. 5 is the depth curve and pitching angle curve when the biorobotic UUV changing depth form 10 to 20 m through changing the central flapping angles of all frontal flapping hydrofoils (Figs. 6 and 7). The simulation results indicate that the biorobotic UUV can steadily complete the motion of change depth through using the two frontal flapping hydrofoils or using all four flapping hydrofoils. The biorobotic UUV can change depth form 10 to 20 m in 300 s through using the two frontal flapping hydrofoils and in 170 s through using all four flapping hydrofoils, so the biorobotic UUV has excellent maneuverability at low velocity, and especially the biorobotic UUV can expedite change depth through all four lapping hydrofoils.

5. Conclusions

The model of biorobotic UUV dimensional motion and the model for fluid dynamics of flapping hydrofoil were presented in this paper for analyzing the dynamics of biorobotic UUV. The simulation results show that:

1) the biorobotic UUV can steadily complete the motion of change depth through using the two frontal flapping hydrofoils or using all four flapping hydrofoils,

2) the biorobotic UUV has excellent maneuverability at low velocity.

References

1. **Menozzi, Alberico; Leinhos, Henry A.; Beal, David N.; Bandyopadhyay**, **Promode R.** 2008. Open-loop control of a multifin biorobotic rigid underwater vehicle [J], IEEE Journal of Oceanic Engineering 33(2): 59-68. http://dx.doi.org/10.1109/JOE.2008.918687.
2. **Mukund Narasimhan; Sahjendra N. Singh** 2006. Adaptive input – output feedback linearizing yaw plane control of BAUV using dorsal fins [J], Ocean Engineering 33: 1413-1430. http://dx.doi.org/10.1016/j.oceaneng.2005.10.004.
3. **Mukund Narasimhan; Sahjendra N. Singh** 2006. Adaptive optimal control of an autonomous underwater vehicle in the dive plane using dorsal fins, Ocean Engineering 33: 404-416. http://dx.doi.org/10.1016/j.oceaneng.2005.04.017.
4. **WANG Zhao-li, SU Yu-min, YANG Liang** 2009. Hydrodynamic analysis of the pectoral-fins in viscous flows, Chinese Journal of Hydrodynamics 24(2): 141-149.
5. **LAO Yi-jia, WANG Zhi-dong, ZHANG Zhen-shan, LI Li-jun** 2009. Experimental measurement and analysis on the wake vortex of oscillating flexible caudal fin, Journal of Hydrodynamics 24(1): 106-112.
6. **LIU Zhen, HYUN Beom-soo, KIM Moo-rong, JIN Ji-yuan** 2008. Experimental and numerical study for hydrodynamic characteristics of an oscillating hydrofoil, Journal of Hydrodynamics 20(3): 280-287. http://dx.doi.org/10.1016/S1001-6058(08)60058-X.
7. **Haibin Xie, Lincheng Shen** 2007. Dynamic analysis on the bionic propulsor imitating undulating fin of aquatic animals, Proceedings of the 2007 IEEE International Conference on Robotics and Biomimetics December 15 -18, Sanya, China, 268-273. http://dx.doi.org/10.1109/ROBIO.2007.4522172.
8. **Shao-bo Yang, Jing Qiu, Xiao-yun Han** 2009. Kinematics modeling and experiments of pectoral oscillation propulsion robotic fish, Journal of Bionic Engineering (6): 174-179. http://dx.doi.org/10.1016/S1672-6529(08)60114-6.
9. **Jeffery S. Riedel** 1999. Seaway learning and motion compensation in shallow waters for small AUVs [D], Ph.D Thesis.
10. **Hai-jun Xu, Cun-yun Pan, Hai-bin Xie, Dai-bing Zhang** 2008. Dynamics modeling and simulation of a bionic swim bladder system in underwater robotics, Journal of Bionic Engineering Supply 66-71.
11. **Cheng Wei, Sun Junling, Dai Jie. Yuan Jianping, Xu Yuru** 2005. Research of bionic underwater vehiele's motion simulation [J], Journal of System Simulation 17(1): 11-15 (in Chinese).
12. **SU Yumin, HUANG Sheng, IKEHATA Mitsuhisa, KAI Hisashi** 2001. Numerical calculation of marine propeller hydrodynamic characteristics in unsteady flow by boundary element method [J], Shipbuilding of China 42(4): 12-22 (in Chinese).

13. **YANG Xiang-hui, YE Heng-kui, FENG Da-kui** 2008. Computational research on wave making of moving wigley hull in time domain, Journal of Hydrodynamics, 20(4): 469-476. http://dx.doi.org/10.1016/S1001-6058(08)60082-7.
14. **Peng Shi** 2004. Underwater bio-robot's motion analysis and animation [D], Master Thesis of Harbin Engineering University, (in Chinese).

DU Xiao-xu, SONG Bao-wei, PAN Guang

BIOROBOTO (UUV) DINAMIKA IR MODELIAVIMAS

R e z i u m ė

Straipsnyje aprašomas bioroboto – automatiškai valdomos povandeninės transporto priemonės (*unmanned underwater vehicle* – UUV) – dinaminis modelis. Į modelį yra įtrauktas naujas, tikslus skystyje panardintos sparnuotės dinaminės sąveikos su skysčiu modelis. Modelis naudojamas bioroboto UUV, kuris kaip kietas kūnas yra stumiamas keturių mentelių, judėjimui modeliuoti. Modeliavimas naudojamas kaip pradinio dizaino priemonė bioroboto UUV manevringumui įvertinti. Modeliavimo rezultatai rodo, kad biorobotas gali nuolat keisti gylį naudodamas dvi priekines arba visas keturias menteles. Biorobotas UUV puikiai manevruoja esant nedideliems greičiams.

DU Xiao-xu, SONG Bao-wei, PAN Guang

DYNAMICS AND SIMULATION OF BIOROBOTIC UUV

S u m m a r y

This paper describes a dynamics model of a biorobotic unmanned underwater vehicle (UUV). And a new accurate model for calculating fluid dynamics of flapping hydrofoil is also incorporated into the simulation. The model is used to simulate the motion of the biorobotic UUV which used a compressed body propelled by four flapping hydrofoils. We use the simulation as a predictive design tool to evaluate the maneuverability of the biorobotic UUV. The simulation results show that the biorobotic UUV can steadily complete the motion of change depth through using the two frontal flapping hydrofoils or using all four flapping hydrofoils. The results also show that the biorobotic UUV has excellent maneuverability at low velocity.

Keywords: biorobotic UUV, fluid dynamics, flapping hydrofoils.

Received April 25, 2012
Accepted September 05, 2013